Mitigation of Jamming Attack in Massive MIMO With One-Bit FBB Sigma-Delta ADCs

Hessam Pirzadeh*, Gonzalo Seco-Granados[†], and A. Lee Swindlehurst*

*Center for Pervasive Communications and Computing, University of California Irvine, Irvine, CA 92697, USA.

Email: {hpirzade, swindle}@uci.edu

[†]Department of Telecommunications and Systems Engineering, Universitat Autònoma de Barcelona. Email: gonzalo.seco@uab.cat

Abstract—We study the uplink performance of a massive multiple-input multiple-output (MIMO) system with one-bit analog to digital converters (ADCs) in the presence of a disruptive jammer. We propose spatial Sigma-Delta $(\Sigma\Delta)$ quantization with an interference cancellation feedback beamformer (FBB $\Sigma\Delta)$ to mitigate the adverse impact of the jammer on the system performance. Then we analyze the performance of this architecture by adopting an appropriate linear model and present a recursive algorithm to calculate the power of the quantization noise. Simulation results show that the spatial FBB $\Sigma\Delta$ architecture can achieve the same symbol error rate as in systems with high-resolution ADCs.

Index Terms—Massive MIMO, one-bit ADCs, sigma-delta, jamming, interference mitigation, beamforming.

I. INTRODUCTION

To decrease the power consumption of massive multipleinput multiple-output (MIMO) systems, architectures with low-resolution analog to digital converters (ADCs) have been studied extensively in the literature [1]- [6]. Although coarse quantization degrades the performance of the system, it has been shown that it can be alleviated by increasing the number of antennas [1] or exploiting more complicated signal processing techniques [7]. Recently, the idea of temporal $\Sigma\Delta$ quantization has been extended to the spatial domain [8]–[11]. It has been shown that, using minimal additional hardware in the analog domain, the resulting spatial one-bit $\Sigma\Delta$ architecture can shape the quantization noise to angles of arrival away from those that correspond to the users of interest. Hence, performance close to that of systems with high-resolution ADCs can be achieved while reducing power consumption and complexity.

One drawback of using one-bit ADCs not addressed in previous work is its susceptibility to strong interference, which can occur in MIMO systems when a jammer is present. Since a one-bit ADC has zero dynamic range, a moderately strong jammer can effectively swamp the relatively weak signals of interest and significantly degrade performance. With one-bit ADCs, jammer mitigation must occur in the RF domain prior

This work was supported by the U.S. National Science Foundation under Grants CCF-1703635 and ECCS-1824565 and by the Spanish Ministry of Science and Universities Grant PRX18/00638.

to sampling, in order for the coarsely quantized ADCs to reveal the dynamics of the signals of interest.

In this paper, we show that the feedback employed by the spatial $\Sigma\Delta$ architecture can be generalized for this purpose. The genesis of the idea comes from work described in [12], which is based on the use of temporally oversampled $\Sigma\Delta$ ADCs. Instead of simply using feedback of the delayed ADC output as in a standard temporal $\Sigma\Delta$ architecture, the approach of [12] employs an analog feedback beamformer (FBB) designed to temporally null the interference. Unlike [12], in the method presented here we take a different approach that does not employ temporal oversampling, but instead uses the spatial $\Sigma\Delta$ architecture. In particular, the feedback between adjacent antennas is generalized to include an FBB signal that also serves to spatially null the interference. We generalize the approach of [11] to develop an equivalent linear model for the $\Sigma\Delta$ array that includes the FBB signal and sets the output level of the one-bit quantizers. Simulations show that while the ordinary spatial $\Sigma\Delta$ architecture is not effective in adequately alleviating the impact of the jammer, our proposed spatial FBB $\Sigma\Delta$ quantizer can provide performance that is close to that of an unquantized system.

In the next section we outline the basic system model. In Section III, some background on temporal FBB $\Sigma\Delta$ modulation is provided and the spatial FBB $\Sigma\Delta$ architecture is proposed. Then we adopt the equivalent linear model developed in [11] to analyze the FBB $\Sigma\Delta$ array. Simulation results are presented in Section IV, followed by our conclusions.

Notation: We use boldface letters to denote vectors, and capitals to denote matrices. The symbols $(.)^*$, $(.)^T$, $(.)^H$, and $(.)^{\dagger}$ represent conjugate, transpose, conjugate transpose, and pseudo inverse, respectively. A circularly-symmetric complex Gaussian (CSCG) random vector with zero mean and covariance matrix \mathbf{R} is denoted $\mathbf{n} \sim C\mathcal{N}(\mathbf{0},\mathbf{R})$. The identity matrix is denoted by \mathbf{I} and the expectation operator by $\mathbb{E}[.]$. For a complex value, $x = x_r + jx_i$, we define $x_r = \Re e[x]$ and $x_i = \Im m[x]$.

II. SYSTEM MODEL

Consider the uplink of a massive MIMO system consisting of a legitimate, single-antenna user that sends its signal to a base station (BS) equipped with a uniform linear array of M

antennas. In addition, a jammer is present that aims to impair the performance of the legitimate user. Accordingly, the $M \times 1$ received signal at the BS is

$$x = \sqrt{p}g_U s_U + n + \sqrt{q}g_J s_J, \tag{1}$$

where p represents the average transmission power from the user, $\mathbf{g}_U = 1/\sqrt{L} \sum_{\ell=1}^L \upsilon_\ell \mathbf{a} \left(\theta_\ell\right)$ is the user's channel vector where L denotes the number of signal paths, $\upsilon_\ell \sim C\mathcal{N}\left(0,1\right)$ is the complex channel gain for the ℓ -th path, and

$$\boldsymbol{a}\left(\theta_{\ell}\right) = \left[1, e^{-j2\pi \frac{d}{\lambda}\sin(\theta_{\ell})}, \cdots, e^{-j(M-1)2\pi \frac{d}{\lambda}\sin(\theta_{\ell})}\right]^{T} \tag{2}$$

denotes the array response vector for angle of arrival θ_ℓ , where d and λ represent the antenna spacing and the carrier wavelength, respectively. The symbol $s_U \in \mathbb{C}$ transmitted from the user satisfies $\mathbb{E}\left[|s_U|^2\right] = 1$, and $\mathbf{n} \sim C\mathcal{N}\left(\mathbf{0}, \sigma_n^2 \mathbf{I}\right)$ denotes additive CSCG receiver noise at the BS. In addition, q represents the jammer's average power, $\mathbf{g}_J = 1/\sqrt{L}\sum_{j=1}^L v_j \mathbf{a}\left(\theta_j\right)$ is the channel vector between the jammer and the BS, and s_J denotes the jammer's signal, where $\mathbb{E}\left[|s_J|^2\right] = 1$.

In a standard implementation involving one-bit quantization, each antenna element at the BS is connected to a one-bit ADC. In such systems, the received baseband signal at the *m*th antenna becomes

$$y_m = Q_m(x_m) , (3)$$

where $Q_m(.)$ denotes the one-bit quantization operation applied separately to the real and imaginary parts as

$$Q_m(x_m) = \alpha_{m,r} \operatorname{sign} (\Re (x_m)) + j\alpha_{m,i} \operatorname{sign} (\Im (x_m)) . \tag{4}$$

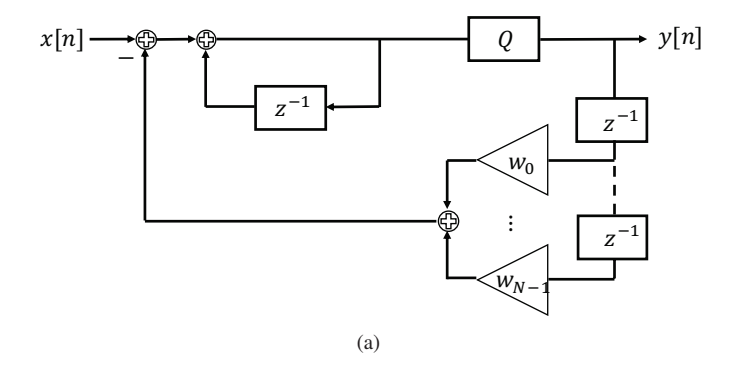
The output voltage levels of the one-bit quantizers are represented by $\alpha_{m,r}$ and $\alpha_{m,i}$. While the value of the output level is irrelevant for standard one-bit quantization, in the case of $\Sigma\Delta$ quantization the selection of adequate output levels is of paramount importance and the necessity for this more general approach will become apparent later¹. Furthermore, we will allow these levels to be a function of the antenna index m, unlike most prior work which assumes that the output levels are the same for all antennas. Finally, the received baseband signal at the BS is given by

$$y = Q(x) = [Q_1(x_1), Q_2(x_2), \cdots, Q_M(x_M)]^T.$$
(5)
III. $\Sigma \Delta$ Architecture

A. Temporal FBB $\Sigma\Delta$ Modulation

In this subsection, we elaborate on the temporal FBB $\Sigma\Delta$ modulation approach of [12] to clarify the noise shaping characteristics of this technique. Fig. 1(a) shows a block diagram representing the *N*th-order temporal FBB $\Sigma\Delta$ modulator with feedback weights $\mathbf{w} = [w_0, \cdots, w_{N-1}]^T$. To shape the quantization noise, the weighted output signals are fed back and subtracted from the input (Δ -stage), and then this error is integrated (Σ -stage).

¹While the one-bit ADC output levels will be optimized, this is a one-time optimization and the values do not change as a function of the user scenario or channel realization. Thus the ADCs are still truly "one-bit."



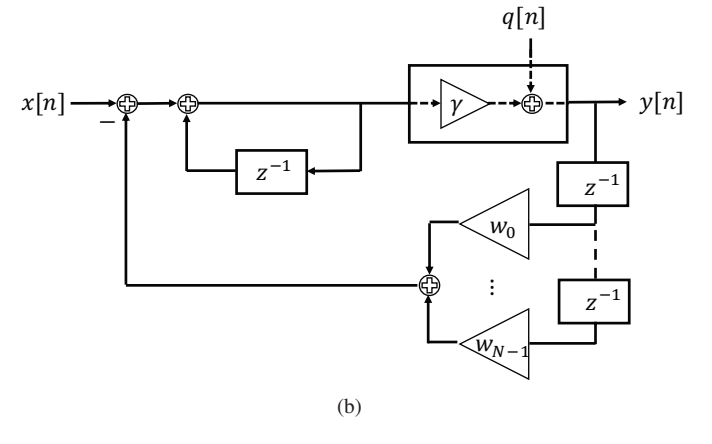


Fig. 1. (a) Block diagram for the Nth-order temporal FBB $\Sigma\Delta$ modulator. (b) Equivalent linear model for the quantizer.

To characterize the transfer function of this non-linear system, we substitute the one-bit quantizer with the equivalent linear model depicted in Fig. 1(b). The input-output relationship of the FBB $\Sigma\Delta$ quantizer can then be written as

$$Y(z) = A(z)X(z) + B(z)Q(z), \tag{6}$$

where $X(z) = \sum_{n=0}^{\infty} x[n] z^{-n}$ denotes the z-transform and

$$A(z) = \frac{\gamma}{1 + (\gamma w_0 - 1) z^{-1} + \gamma w_1 z^{-2} + \dots + \gamma w_{N-1} z^{-N}}$$
 (7)

$$B(z) = \frac{1 - z^{-1}}{1 + (\gamma w_0 - 1) z^{-1} + \gamma w_1 z^{-2} + \dots + \gamma w_{N-1} z^{-N}}.$$
 (8)

Unlike ordinary $\Sigma\Delta$ modulation that passes the signal through an all-pass filter and the quantization noise through a high-pass filter, in (6) we see that X(z) is passed through A(z) and Q(z) through B(z) for FBB $\Sigma\Delta$ modulation. Hence, this approach not only provides a tool for shaping the quantization noise, but proper design of the feedback weights w allows for temporal filtering that passes the desired signal while eliminating undesirable contributions from other sources such as a jammer.

B. One-Bit Spatial FBB $\Sigma\Delta$ Modulation

The idea underlying temporal FBB $\Sigma\Delta$ modulation can be adapted to the angle domain, in order to *spatially* shape the quantization noise in a desired way and remove interference. Instead of forming the Δ component using delayed

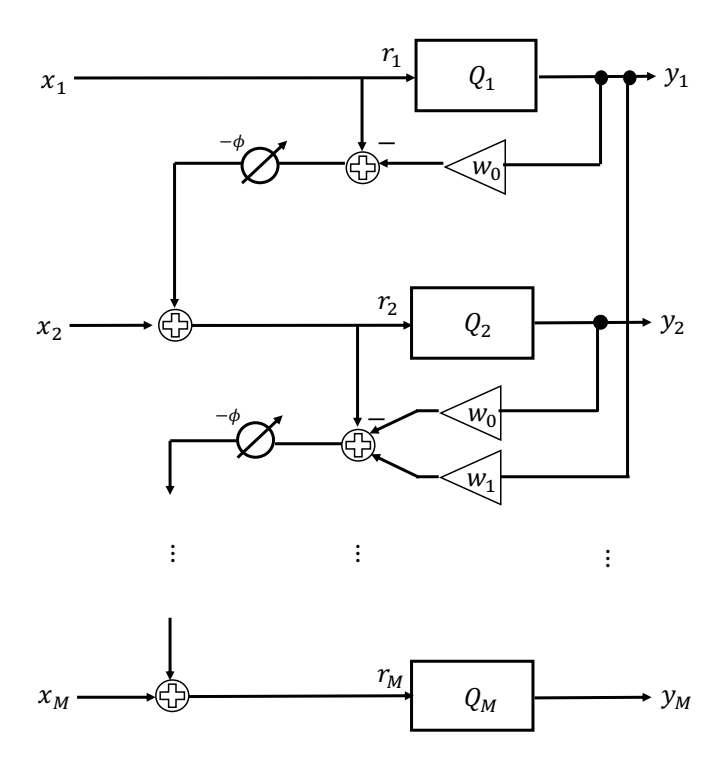


Fig. 2. Spatial FBB $\Sigma\Delta$ architecture.

samples of the quantized input as in the temporal case, we use the quantized signals from adjacent antennas. A direct translation of the temporal $\Sigma\Delta$ concept to the angle domain pushes the quantization noise to higher spatial frequencies, which correspond to angles away from the array broadside $(|\theta| \gg 0^{\circ})$, while oversampling (i.e., reduced d/λ) pushes the signals of interest near broadside closer to zero spatial frequency. However, by phase-shifting the quantization error in the feedback loop prior to the Σ stage, the quantization error can be shaped away from a band of spatial frequencies that is not centered at zero. This bandpass approach has been proposed for spatial $\Sigma\Delta$ architectures in [9], [11]. It is worthwhile to note that although ordinary $\Sigma\Delta$ modulation provides a noise shaping characteristic, FBB $\Sigma\Delta$ not only shapes the quantization noise, but also suppresses the extra quantization noise caused by the jammer with appropriate feedback beamforming.

Fig. 2 shows the architecture of the angle-steered FBB $\Sigma\Delta$ array. Using Fig. 2, we can formulate a compact input-output description of the spatial FBB $\Sigma\Delta$ array by defining

$$U = \begin{bmatrix} 1 & & & & & \\ e^{-j\phi} & 1 & & & & \\ \vdots & \ddots & \ddots & & \\ e^{-j(M-1)\phi} & \cdots & e^{-j\phi} & 1 \end{bmatrix}$$
(9)

$$V = e^{-j\phi} \mathbf{Z}_{-1} U W, \tag{10}$$

where²

$$\mathbf{Z}_{-1} = \begin{bmatrix} 0 & & & & \\ 1 & 0 & & & \\ \vdots & \ddots & \ddots & & \\ 0 & \ddots & 1 & 0 \end{bmatrix}$$
 (11)

and expressing the input to the quantizers as

$$r = Ux - Vy. (13)$$

The output of the angle-steered one-bit FBB $\Sigma\Delta$ array is then defined by

$$y = Q(r). (14)$$

To analyze the performance of spatial $\Sigma\Delta$ processing, we will represent the one-bit quantization operation in (14) with an equivalent linear model [11]

$$y = Q(r) = \Gamma r + q, \tag{15}$$

where $\Gamma = \operatorname{diag}(\gamma_1, \ldots, \gamma_M)$ with

$$\gamma_{m} = \frac{\mathbb{E}\left[r_{m}y_{m}^{*}\right]}{\mathbb{E}\left[\left|r_{m}\right|^{2}\right]} = \alpha_{m} \frac{\mathbb{E}\left[\left|\Re \left[r_{m}\right]\right| + \left|\Im \left[r_{m}\right]\right|\right]}{\mathbb{E}\left[\left|r_{m}\right|^{2}\right]},$$
 (16)

and q denotes the effective quantization noise. In (16), it is assumed that r_m is circularly symmetric. This assumption implies that identical values should be selected for the output levels of the real and imaginary quantizers, and thus we will let α_m represent both $\alpha_{m,r}$ and $\alpha_{m,i}$. Following the same reasoning as in [11], we will set $\Gamma = I$ by choosing an appropriate value for each α_m . Therefore, we obtain the following mathematical model for the FBB $\Sigma\Delta$ architecture:

$$y = B^{-1}Ux + B^{-1}q, (17)$$

where B = I + V. Equation (17) is the spatial equivalent of the temporal FBB $\Sigma\Delta$ description in (6), with the following equivalences:

$$\mathbf{B}^{-1}\mathbf{U} \longleftrightarrow A(z) \tag{18}$$

$$\mathbf{B}^{-1} \longleftrightarrow B(z).$$
 (19)

Note that the condition $\Gamma = I$ and assuming that r_m is approximately Gaussian leads to the following choice for the output levels [11]:

$$\alpha_m^{\star} = \frac{\sqrt{\pi \mathbb{E}\left[|r_m|^2\right]}}{2}.\tag{20}$$

 2 Note that \mathbf{Z}_{-1} is the spatial domain equivalent of the delay operator z^{-1} for the z-transform in the time domain.

Next, we calculate the power of the equivalent quantization noise q, which is needed both to analytically assess the system performance and to compute α_m^* . In the discussion below, we show how to express (20) in terms of the statistics of the array input x, which illustrates how the quantizer output levels can be analytically chosen in a practical setting. Moreover, we will show how spatial FBB $\Sigma\Delta$ impacts the power of the quantization noise and elaborate on how it differs from the ordinary spatial $\Sigma\Delta$ approach.

With $\Gamma = I$, (15) becomes

$$y = r + q. (21)$$

Since r_m and q_m are uncorrelated, and using (20), we obtain

$$\mathbb{E}\left[|q_m|^2\right] = \mathbb{E}\left[|y_m|^2\right] - \mathbb{E}\left[|r_m|^2\right] = \left(\frac{\pi}{2} - 1\right)\mathbb{E}\left[|r_m|^2\right]. \tag{22}$$

To determine $\mathbb{E}[|r_m|^2]$, we substitute (21) into (13), so that

$$\boldsymbol{r} = \boldsymbol{B}^{-1} \boldsymbol{U} \boldsymbol{x} - \boldsymbol{B}^{-1} \boldsymbol{V} \boldsymbol{q}. \tag{23}$$

Let us denote $\Psi = B^{-1}U$ and $\Upsilon = B^{-1}V$. It is clear that Ψ is a lower triangular matrix and Υ is a lower triangular matrix with zeros along the main diagonal. In addition, following the same reasoning as in Appendix A of [1], it can be shown that $\mathbb{E}\left[x_{m'}q_m^*\right] \approx 0$, $\forall m,m' \in \mathcal{M} = \{1,\cdots,M\}$. This results in $R_{qx} \approx 0$. Therefore,

$$\mathbf{R}_{r} \approx \mathbf{\Psi} \mathbf{R}_{x} \mathbf{\Psi}^{H} + \mathbf{\Upsilon} \mathbf{R}_{a} \mathbf{\Upsilon}^{H} . \tag{24}$$

Eq. (24) implies that

$$\mathbb{E}\left[|r_{m}|^{2}\right] \approx \begin{cases} \left[\Psi R_{x} \Psi^{H}\right]_{mm} & m = 1\\ \left[\Psi R_{x} \Psi^{H}\right]_{mm} + \left[\Upsilon R_{q} \Upsilon^{H}\right]_{mm} & m > 1 \end{cases}$$
(25)

To approximate $\mathbb{E}\left[|r_m|^2\right]$, and for the sake of analysis, we assume R_q is diagonal. Since Υ is a lower triangular matrix with zeros along the main diagonal, we only need the first m-1 diagonal elements of R_q to specify $\mathbb{E}\left[|r_m|^2\right]$. Hence, we can recursively calculate $\mathbb{E}\left[|r_m|^2\right]$ for m>1 using (22) and (25). In the next section, we show that the diagonal elements of R_q are much smaller than those for the ordinary $\Sigma\Delta$ architecture. This is because of the appropriate design of the feedback weights that lead to the elimination of strong interference before the one-bit quantization.

IV. NUMERICAL RESULTS

This section describes the results of several Monte Carlo simulations in order to illustrate the performance of the FBB $\Sigma\Delta$ quantizer. In our simulations, we assume L=20 multipath arrivals for both the legitimate user and the jammer with angles of arrival randomly uniformly distributed in $\theta_l \in [\theta_0 - \delta, \theta_0 + \delta]$, where the center angle θ_0 is different for the user and the jammer. We set $\theta_{0u} = -20^\circ$ and $\theta_{0j} = 60^\circ$ for the desired user and jammer, respectively, with $\delta = 5^\circ$. We further assume $d/\lambda = 1/4$, 8-PSK symbols, and 10^5 trials. The steering angle of the FBB $\Sigma\Delta$ array is set to $\phi = 2\pi \frac{d}{\lambda}\sin{(\theta_{0u})}$. We let $\sigma_n^2 = 1$, so that p and q denote the SNR of the user and the jammer, respectively. In all simulations, we consider a strong

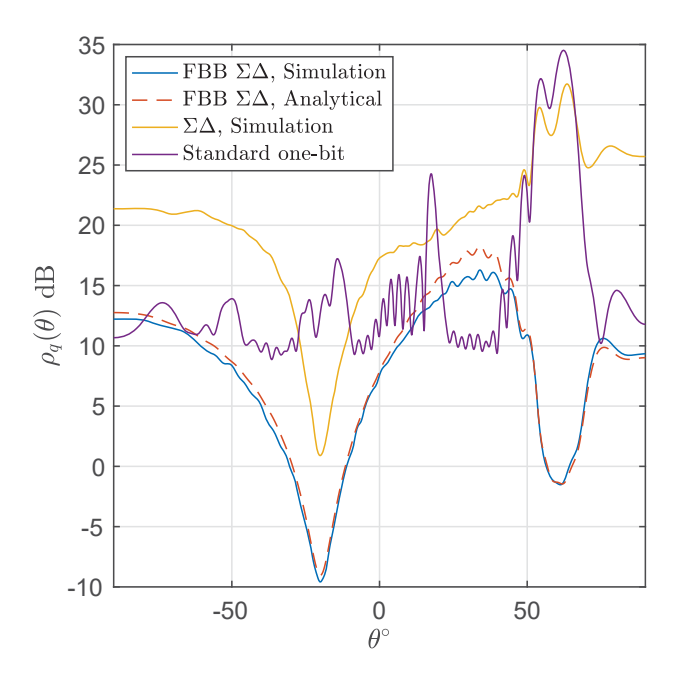


Fig. 3. Spatial spectrum of the quantization noise for the FBB $\Sigma\Delta$, regular $\Sigma\Delta$, and standard one-bit architectures when $d=\lambda/4$, p=0 dB, q=20 dB, and N=50.

interference setting with q = 20 dB. We also assume that θ_{0u} and θ_{0j} are known at the BS³. Hence, following the same reasoning as in [12], the feedback weights are estimated as

$$\mathbf{w} = \left(e^{-j\phi}\mathbf{Z}_{-1}U\bar{\mathbf{Y}}\right)^{\dagger}(U\bar{\mathbf{x}} - \bar{\mathbf{y}}),\tag{26}$$

where

$$\bar{\mathbf{Y}} = \begin{bmatrix}
\bar{y}_0 & \mathbf{0} \\
\bar{y}_1 & \ddots \\
\vdots & \ddots & \bar{y}_0 \\
\vdots & \vdots & \vdots \\
\bar{y}_{M-1} & \cdots & \bar{y}_{M-N}
\end{bmatrix}, \ \bar{\mathbf{y}} = \beta \mathbf{a} \left(\theta_{0u}\right) \tag{27}$$

$$\bar{\mathbf{x}} = \beta \mathbf{a} \left(\theta_{0_u} \right) + \mathbf{a} \left(\theta_{0_j} \right). \tag{28}$$

and β is a constant. In the simulations that follow, we selected $\beta = \sqrt{10}$. Then, the solution in (26) is followed by iterative refinement (see Section III-C in [12]) to find the desired feedback weights.

Fig. 3 shows the simulated and analytically derived quantization noise power density which is defined as

$$\rho_{q}(\theta) \triangleq \frac{1}{M} \boldsymbol{a}(\theta)^{H} \boldsymbol{R} \boldsymbol{a}(\theta), \tag{29}$$

where R is the covariance matrix of the quantization noise for each approach (standard one-bit, $\Sigma\Delta$, or FBB $\Sigma\Delta$). In this

³Note that, although here we consider a single jammer in a known location, the feedback weights can in general be designed to reduce the impact of signals arriving from multiple sectors in which the jammers are known to lie, without precise knowledge of the actual jammer locations.

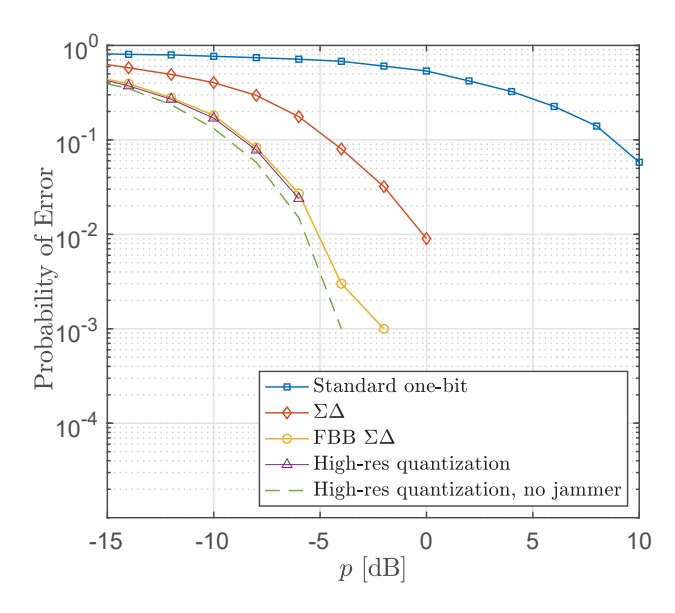


Fig. 4. Symbol error rate versus p for a system with $\theta_{0u}=-20^\circ$ and $\theta_{0i}=60^\circ$, $d=\lambda/4$, q=20 dB, N=50.

figure, we set the order of the FBB $\Sigma\Delta$ filter at N=50. We see that the quantization noise power for the FBB $\Sigma\Delta$ array is substantially lower over the angles where the user is present, while the effect is the opposite for standard one-bit quantization – the quantization noise is higher for angles where the amplitude of the received signals is larger. In addition, we see that even the ordinary $\Sigma\Delta$ array suffers from large quantization noise in the presence of strong interference. We also observe that there is excellent agreement between the simulations and our theoretically derived expressions for both cases. Note that careful design of the quantizer output levels is a critical component in achieving the desired $\Sigma\Delta$ noise shaping characteristic shown here.

In Fig. 4, we compare the symbol error rate of the FBB $\Sigma\Delta$ array with that of a system with high-resolution ADCs and a system with high-resolution ADCs and no strong interference, i.e., $x_p = \sqrt{p} g_U s_U + n$, as a benchmark. The methods that do not allow FBB in the RF domain must attempt to cancel the interference digitally, after the quantization. Consequently, for the systems implemented with high-resolution ADCs, standard one-bit ADCs, and the original spatial $\Sigma\Delta$ architecture, we project the sampled signal onto the subspace orthogonal to the interference in the digital domain. Denoting the signals received by the standard one-bit and $\Sigma\Delta$ architectures by y_1 and $y_{\Sigma\Lambda}$, respectively, the signals after the projection for the three methods are given by $B^{-1}Ux$, $B^{-1}Uy_1$, and $B^{-1}Uy_{\Sigma\Delta}$. We assume perfect channel state information (CSI) is available and use the maximum ratio combiner (MRC) at the BS to decode the 8-PSK symbols. Fig. 4 shows the superior performance of the one-bit FBB $\Sigma\Delta$ architecture which achieves performance equivalent to that of a system with only high resolution ADCs. This performance is achieved with only minimal additional hardware in the analog domain, and thus has significantly reduced complexity and energy consumption compared with a system employing high-resolution ADCs.

V. CONCLUSION

We presented a new spatial one-bit FBB $\Sigma\Delta$ architecture for mitigating strong interference in massive MIMO systems with one-bit quantization. We showed that this simple architecture can effectively compensate for the vulnerability of one-bit ADCs against strong interference. The critical challenges in designing this architecture are to find the appropriate output levels for the one-bit quantizers and the values for the feedback weights. A recursive algorithm was proposed to specify the quantizers' output levels. The feedback weights were designed by adopting an algorithm used previously for a temporal FBB $\Sigma\Delta$ implementation. However, the behaviour of the feedback weights indicates that they amount to a spatial beamformer pointing in the direction(s) of the interference, and hence could be designed by a less complicated approach. Interesting directions for future work include studying the impact of angle estimation errors on the performance of the FBB $\Sigma\Delta$ architecture, or using the approach for combined quantization noise shaping and transmit beampattern design for the downlink with low-resolution digital-to-analog converters.

REFERENCES

- Y. Li, C. Tao, L. Liu, A. Mezghani, G. Seco-Granados, and A. Swindlehurst, "Channel estimation and performance analysis of one-bit massive MIMO systems," *IEEE Trans. Signal Process.*, vol. 65, no. 15, pp. 4075-4089, May 2017.
- [2] C. Mollen, J. Choi, E. G. Larsson, and R. W. H. Jr, "Uplink performance of wideband massive MIMO with one-bit ADCs," *IEEE Trans. Wireless Commun.*, vol. 16, no. 1, pp. 87-100, Jan. 2017.
- [3] C. Studer and G. Durisi, "Quantized massive MU-MIMO-OFDM uplink," IEEE Trans. Commun., vol. 64, no. 6, pp. 2387–2399, June 2016.
- [4] J. Mo and R. W. Heath, "Capacity analysis of one-bit quantized MIMO systems with transmitter channel state information," *IEEE Trans. Signal Process.*, vol. 63, no. 20, pp. 5498–5512, Oct. 2015.
- [5] N. Liang, W. Zhang, "Mixed-ADC massive MIMO," IEEE J. Sel. Areas in Commun., vol. 34, no. 4, pp. 983-997, April 2016.
- [6] H. Pirzadeh, and A. Swindlehurst, "Spectral efficiency of mixed-ADC massive MIMO," *IEEE Trans. Signal Process.*, vol. 66, no. 13, pp. 3599-3613, July 2018.
- [7] J. Choi, J. Mo, and R. W. Heath, "Near maximum-likelihood detector and channel estimator for uplink multiuser massive MIMO systems with one-bit ADCs," *IEEE Trans. Commun.*, vol. 64, no. 5, pp. 2005–2018, May 2016.
- [8] R. M. Corey and A. C. Singer, "Spatial sigma-delta signal acquisition for wideband beamforming arrays," in *Proc. Int. ITG Workshop Smart Antennas (WSA)*, March 2016.
- [9] M. Shao, W. K. Ma, Q. Li, and A. Swindlehurst, "One-Bit Sigma-Delta MIMO Precoding," *IEEE J. Sel. Topics Signal Process.*, vol. 13, no. 5, pp. 1046-1061, Sep. 2019.
- [10] S. Rao, A. Swindlehurst, and H. Pirzadeh, "Massive MIMO channel estimation with 1-bit spatial sigma-delta ADCs," in *IEEE International* Conf. on Acoustics, Speech and Signal Processing (ICASSP), Brighton, UK, May 2019.
- [11] H. Pirzadeh, G. Seco-Granados, S. Rao, and A. Swindlehurst, "Spectral efficiency of one-bit ΣΔ massive MIMO," arXiv.org Oct. 2019. Available: http://arxiv.org/abs/1910.05491.
- [12] V. Venkateswaran, and A. J. van der Veen, "Multichannel ΣΔ ADCs with integrated feedback beamformers to cancel interfering communication signals," *IEEE Trans. Sig. Process.*, vol. 59, no. 5, pp. 2211-2222, May 2011.